Numerical studies of steel-concrete-steel sandwich walls with J-hook connectors subjected to axial loads

Zhenyu Huang [*1] and J.Y. Richard Liew [2a]

[1] *Department of Civil and Environmental Engineering, National University of Singapore,*
E1A-07-03, 1 Engineering Drive 2, 117576 Singapore
[2] *College of Civil Engineering, Nanjing Tech University, Nanjing, Jiangsu, 211816 China*

Abstract. Steel-concrete-steel (SCS) sandwich composite wall has been proposed for building and offshore constructions. An ultra-lightweight cement composite with density 1380 kg/m^3 and compressive strength up to 60 MPa is used as core material and inter-locking J-hook connectors are welded on the steel face plates to achieve the composite action. This paper presents the numerical models using nonlinear finite element analysis to investigate the load displacement behavior of SCS sandwich walls subjected to axial compression. The results obtained from finite element analysis are verified against the test results to establish its accuracy in predicting load-displacement curves, maximum resistance and failure modes of the sandwich walls. The studies show that the inter-locking J-hook connectors are subjected to tension force due to the lateral expansion of cement composite core under compression. This signifies the important role of the interlocking effect of J-hook connectors in preventing tensile separation of the steel face plates so that the local buckling of steel face plates is prevented.

Keywords: finite element; J-hook connector; sandwich wall; steel-concrete-steel; ultra-lightweight cement

1. Introduction

Steel-Concrete-Steel (SCS) sandwich composite panels are structural elements that comprise two external steel plates infilled with a concrete core. The SCS sandwich composite exhibits significant structural and economic advantages over the conventional reinforced concrete structures in terms of flexural stiffness, resistance and energy absorption capacity to withstand extreme environmental and accidental loads. The external steel plates serve as a permanent formwork during concreting, promoting construction efficiency and reducing the site handling costs and time. The external steel plates prevent sea water intrusion into the concrete core and reduce the surface area needed for corrosion coating making it easy for inspection and maintenance. Therefore, SCS sandwich composite structures can be adopted as heavy duty and protective structural applications such as ship hulls, tunnels, military barriers and nuclear power station walls that require high resistance against extreme loads (Epackachi *et al.* 2015, Remennikov *et al.* 2013, Marshall *et al.* 2012, Zhang *et al.* 2014, Huang *et al.* 2015a, b). The composite action between the steel plates and concrete core can be achieved by using mechanical

∗Corresponding author, Research Fellow, Ph.D., E-mail: zhenyu_huang@nus.edu.sg
[a] Ph.D., Professor, E-mail: ceeljy@nus.edu.sg

connectors or adhesive materials (Xie *et al*. 2004, Xu and Sugiura 2013, Aboobucker *et al*. 2009). The use of mechanical connectors are more reliable than adhesive to resist the longitudinal slip and prevent tensile separation between the steel plate and concrete core.

Past research on flat SCS sandwich composite panels have paved a better understanding of the structural behavior subject to lateral static and dynamic loads. Liew and Sohel (2009) and Sohel and Liew (2011) carried out tests and nonlinear finite element analysis of SCS sandwich beams with J-hook connectors and lightweight concrete to investigate their static behavior and load resistance performance. Analytical methods to predict the maximum resistance were proposed and verified against the numerical and tests results. Additional work on SCS sandwich flat panels subject to lateral impact and blast loads were also carried out to demonstrate their superior structural performance, engineering flexibility and construction economy for application as protective barriers (Liew *et al*. 2009, Liew and Wang 2011, Remennikov *et al*. 2013, Sohel and Liew 2014).

A comprehensive review of the published literature reveals that the majority of the research work has been focused on experimental investigation to establish analytical methods for design implementation. Although physical testing provides valuable information on the overall performance of SCS sandwich composite beams and slabs and the local behavior of constituent materials, high costs associated with full scale testing often place a limit on the range of parameters to be investigated.

Numerical analysis using Finite Element Method (FEM) is becoming increasingly popular and provides a cost-effective tool for carrying out full scale simulation on steel-concrete composite structures (Hu and Nie 2015, Smitha and Kumar 2013). The nonlinear behavior of steel, concrete and reinforced bar or shear connectors can be taken into consideration by incorporating appropriate constitutive laws and iterative procedures. FEM can reproduce a thorough structural response under different load scenarios such as displacement, stress, strain and concrete crack development history, etc. A proper calibrated FE model is useful to provide an in-depth understanding of the structural behavior of the steel-concrete composite structures. Nonetheless, only a limited amount of research is available on the experimental work of SCS sandwich wall structures with shear connectors (Zhang *et al*. 2014, Choi *et al*. 2014). Calibration of numerical model are not well established especially for structures that involve new materials and new connectors. The lack of FE studies may be partially due to the challenging nature of modelling the interface between different new constituent materials including lightweight cement composite, steel plates, shear studs and their interactions.

The usual methods in modelling the shear connector in concrete are: (1) embedment of shear connectors in concrete element in which the connector part and concrete part share the nodes following the strain compatibility rule. This model is straightforward in modelling but ignores the slip between the concrete and connectors and it may overestimate the stiffness of the structure; and (2) modeling the surface contact between concrete and connectors. Using this method, Nguyen and Kim (2009) and Xie *et al*. (2004) proposed an accurate nonlinear FE model which took into account the nonlinear properties of the concrete, steel beam, reinforcement bars and connectors to investigate the push-out capacity of shear connectors embedded in concrete. This model is more accurate than the first one but it involves high computational cost and may face convergence problem when modelling large-scale structure with many connectors.

Another simplified FE model was proposed for the SCS sandwich structure with overlapped headed shear studs by Shanmugam *et al*. (2002) and Zhang *et al*. (2014) in which they modelled the shear connectors as 2-D or 3D springs acting in series to represent the behavior of shear

connector. This simplification significantly reduces the difficulty of modelling the overlapped shear connectors in the concrete core and reduces the total amounts of the elements. However, the spring analogy ignores the complex interaction between concrete and studs. This model did not consider concrete bearing failure and could not capture the true failure behavior of shear connectors.

The numerical models proposed by various researchers were meant for quasi-static analysis and focused on conventional composite columns and beams (Dabaon *et al.* 2009, Wang *et al.* 2012, Long and Cai 2013). Concrete confinement effect and local buckling of steel plates were investigated. There is no published information on numerical modelling of compressive behavior of SCS sandwich walls with through connectors and lightweight concrete core.

In SCS sandwich composite wall with J-hook connectors, the J-hook connectors that work in pairs and interlock each other are used to transfer interfacial shear force, resist tensile force due to outward concrete expansion and prevent local buckling of the steel face plates. Since their roles in SCS sandwich structures are significant, it is necessary to capture their detailed behavior in the FE analysis. This paper proposes an effective FE model to investigate the compressive behavior of SCS sandwich walls infilled with lightweight cement composite subjected to axial compression. A three-dimensional nonlinear FE model is established for SCS sandwich composite walls using the explicit code in ABAQUS (2013). This model takes into appropriated account of the material nonlinearity, and the interaction between concrete, steel and shear connectors. Fifteen SCS sandwich wall specimens tested under compressive load have been analyzed by the FE model. The maximum compressive resistance, load-shortening curves, failure modes and the extent of damage in the cement core are compared with the corresponding experimental results to verify the accuracy of the proposed FE model.

2. Experimental investigation

A series of tests on SCS sandwich walls with J-hook shear connectors were carried out by the authors (Huang and Liew 2016a, b, Huang *et al.* 2015a). The wall specimens, having core depth from 90 to 132 mm, length from 400 mm (short wall) to 2500 mm (slender wall), and width 590 mm are subjected to axial compression, as shown in Fig. 1. The compression tests were carried out


(a) Front view (*H* = 400-2500 mm, *t_s* = 6, 8, 12 mm, *h_c* = 90, 120, 132 mm, *s* = 100, 200, 300 mm, *s'* = 50 mm)   (b) A-A
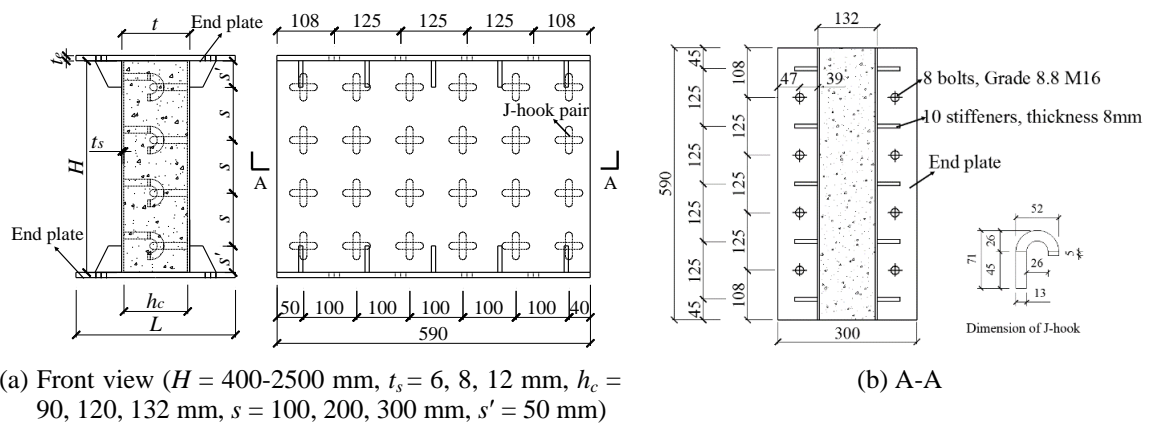
Fig. 1 Dimensions of typical SCS sandwich wall specimens

(a) Schematic of test setup   (b) Test specimen SCSW-S1
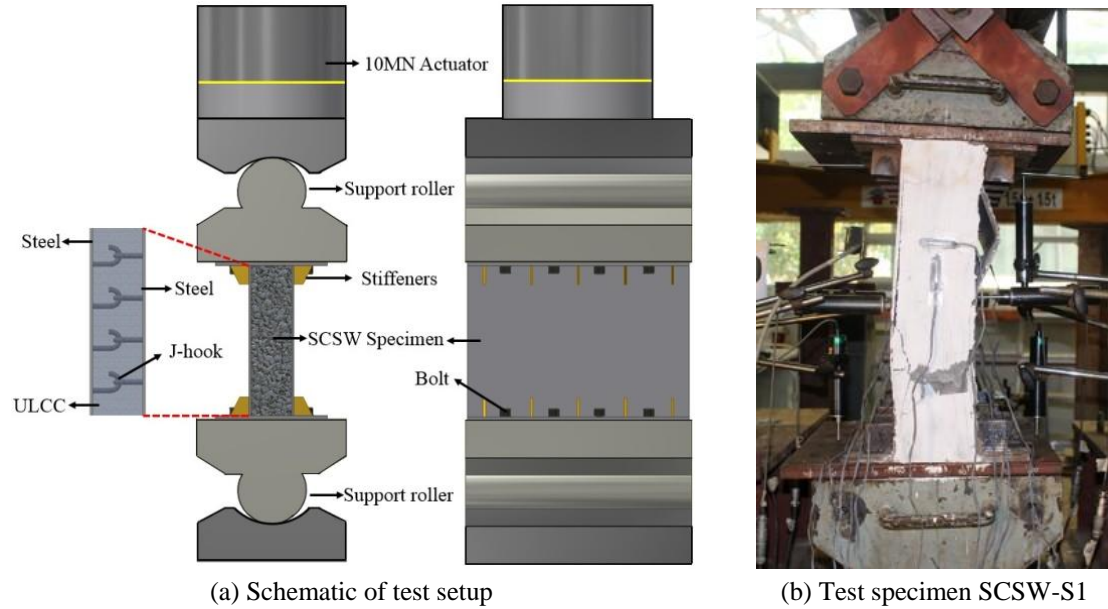
Fig. 2 Test setup and SCS sandwich wall specimen

Table 1 Dimension of sandwich wall specimens

Specimen	Specimen size				s (mm)	Connector	s/t_s	λ	f_{ck} (MPa)	f_y (MPa)
	H (mm)	W (mm)	h_c (mm)	t_s (mm)						
SCSW-R1	400	590	120	6.0	100		16.67	0.29	54.3	309.4
SCSW-R2	400	590	120	6.0	100		16.67	0.29	54.3	309.4
SCSW-H1	1000	590	120	5.0	100		20.00	0.51	60.9	309.4
SCSW-H2	2500	590	120	6.0	100		16.67	0.92	58.9	309.4
SCSW-S1	500	590	120	6.0	201		33.50	0.32	54.6	309.4
SCSW-S2	700	590	120	6.0	300		50.00	0.38	55.0	309.4
SCSW-C1	400	590	90	6.0	100	J-hook	16.67	0.37	60.0	309.4
SCSW-C30	400	590	120	6.0	100		16.67	0.27	37.8	309.4
SCSW-C45	400	590	120	6.0	100		16.67	0.29	54.4	309.4
SCSW-T8	400	590	120	8.0	100		12.50	0.30	57.1	393.9
SCSW-T12	400	590	120	12.0	102		8.50	0.25	52.0	375.0
SCSW-P1	400	590	120	6.0	103		17.17	0.30	55.3	309.4
SCSW-P2	400	590	120	6.0	100		16.67	0.29	53.8	309.4
SCSW-C2	400	590	135	6.0	100		16.67	0.26	52.6	309.4

*H = height of specimen; t_s = thickness of steel plate; W = width of sandwich wall section; s = spacing of connector; s/t_s = plate slenderness ratio; $\lambda = \sqrt{N_{pl,Rk} / N_{cr}}$; f_{ck}= compressive strength of concrete cylinder $\emptyset 100 \times 200$; f_y = yield strength of steel

using a 10 MN Instron testing actuator operated in displacement-control mode, as shown in Fig. 2(a). The wall specimens were loaded at a rate of 0.2 mm/min. The nominal thickness of the face plates was 6 mm. The J-hook connectors were fabricated from round steel bar of diameter 13 mm. To investigate the composite action, the spacing of J-hook connectors was varied from 100 mm to 300 mm. The walls were instrumented by LVDTs and strain gauges to measure deflections and strains of steel plates respectively. A new type of ultra-lightweight cement composite with density 1380 kg/m^3 and compressive strength up to 60 MPa was used to produce the concrete core for the sandwich walls. The cement composite was reinforced with 0.5% PVA fibres. The detailed dimensions of walls, concrete strength and yield strength of steel are shown in Table 1.

Test results showed that J-hook shear connectors were effective in preventing tensile separation of the steel face plates, thus reducing the chance of plate buckling and maintaining the structural integrity despite the presence of compressive and splitting cracks in the concrete core. The main failure modes of short sandwich walls were: (1) concrete crushing followed local buckling of steel plate, as shown in Fig. 3(a); and (2) cross-sectional failure, shown in Fig. 3(b). The walls with larger spacing of shear connectors typically failed by local buckling of face plates. Significan buckling of steel face plate was observed for the walls with partial strength connectors, as shown in Fig. 3(c). The slender sandwich wall that failed in global buckling experienced less damage on the concrete core but with a small damage zone near the mid-height of the wall, showing the local concrete crushing and local buckling of plate (Fig. 3(d)). The ultra-lightweight concrete core exhibited brittle behavior and cracked into many pieces after failure.
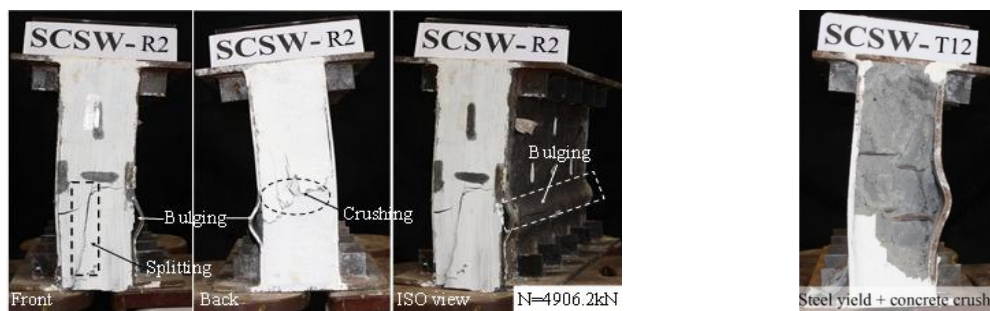

(a) Concrete crushing and plate buckling   (b) Cross-sectional failure
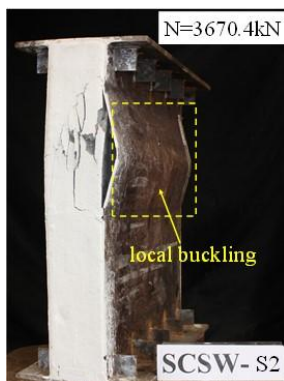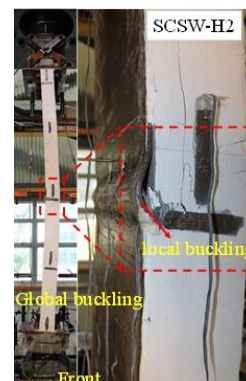
(c) Local buckling of steel plates   (d) Global buckling of slender wall

Fig. 3 Typical failure modes of sandwich wall
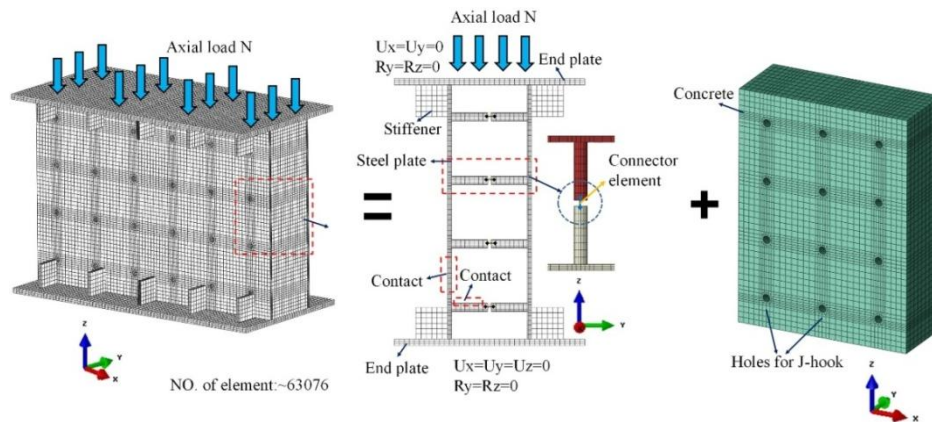
Fig. 4 Typical FE model for SCS sandwich wall

3. Numerical modelling

3.1 Sandwich wall

Fig. 4 depicts a typical FE model of the sandwich wall under compression. The steel face plate, J-hook connectors and concrete core are meshed with C3D8R solid elements. In the finite element modelling, the geometry of the steel plates and connectors are divided into regular zones to obtain uniform mesh distribution. The maximum average aspect ratio of each three-dimensional solid continuum element is set to be 2.0. The mesh size for the continuum element of 10 mm is used. Taking specimen SCSW-R1 as an example, there are 42532, 6144 and 14400 elements for the outer steel plate, connectors and concrete core, respectively.

Surface-to-surface contact option is applied to model the contact interfaces between steel plates and concrete, and hook surface and concrete core. This algorithm generates slave (concrete) and master surfaces (steel). For two deformable surfaces in contact, the master surface refers to the stiffer body or the surface with a coarser mesh if the two surfaces have comparable stiffness. Penalty method is used for handling the contact phenomenon where normal interface springs are used to resist interpenetration between element surfaces. The interface stiffness is computed as a function of the bulk modulus, volume and face area of the elements on the contact surface. A friction coefficient should be defined. Some researchers have suggested the friction coefficient ranges from 0.2-0.6 (Seifi and Abbasi 2015, Rahman and Kong 2012, Li *et al*. 2014). A sensitivity analysis has been carried out using friction coefficient 0.2 to 0.6 and the results show that the friction coefficient leads to little difference in both overall load-shortening response and failure mode (Huang and Liew 2015). The difference in the predicted maximum load obtained is less than 5%. Therefore, the friction coefficient value 0.5 is used. The normal behavior adopts a hard contact relationship. The coincident nodes between the elements of steel face plate and J-hook shear connectors are merged in the FE model to simulate a perfect weld condition.

3.2 Material model

3.2.1 Concrete
The Concrete Damage Plasticity (CDP) model available in ABAQUS is employed to model the nonlinear behavior of lightweight cement composite. It allows the definition of strain hardening in

compression and can be defined to be sensitive to the strain rate, which resembles the behavior of concrete more realistically. The CDP model consists of the combination of nonassociated multi-hardening plasticity and scalar (isotropic) damaged elasticity to describe the irreversible damage that occurs during the fracturing process. It is designed for applications in which concrete is subject to monotonic, cyclic and dynamic loading under low confining pressures and it can consider the main failure mechanisms of concrete crushing and cracking for both ABAQUS/Standard and Explicit solvers. The CDP model has been applied to simulate the concrete behavior in steel-concrete composite structures and the FE models were verified against those published test data (Zheng *et al*. 2009, Zhang *et al*. 2014, Nguyen and Kim 2009). The mechanical properties of ULCC obtained from the tests, as shown in Table 2, and used in the FEM model. The typical uniaxial stress-strain curves for ULCC is used to calculate the parameters in the CDP model as shown in Fig. 5.

Since ULCC is a new type of lightweight cement grout with limited information available on its constitutive relationship, the present study calibrates the parameters of CDP model based on the test data. The experimental stress-strain behavior of concrete in tension and compression are used as input parameters for the damaged plasticity model. The damage parameters d_c and d_t employed in concrete compression hardening and tension stiffening curves can be calibrated through uni-axial compression and four-point bending tests. Based on the verification in ABAQUS, Wang and Chen (2006) concluded that a first-order exponential decay function can describe the damage mode of concrete which showed that the compressive normalised damage variable $D_{c,norm}$ was related to normalised compressive inelastic strain $\varepsilon_{c,norm}^{in}$. This relation takes the following form

$$D_{c,norm} = A_0 e^{-\varepsilon_{c,norm}^{in}/t_0} + B_0 \tag{1}$$

where, $D_{c,norm} = d_c$, $\varepsilon_{c,norm}^{in} = \varepsilon_c^{in}/\varepsilon_{cm}$, $\varepsilon_c^{in} = \varepsilon_c - \sigma_c/E_0$, $A_0 = 1/(e^{-1/t_0} - 1)$, $B_0 = -1/(e^{-1/t_0} - 1)$. The only unknown parameter t_0 can be determined by fitting the uni-aixal stress-strain curves from simulation with the experimental test. Similarly, the relation between normalised tensile damage

Table 2 Material properties of ULCC

Age (28d) Cylinders	ρ_w (kg/m³)	Compression Strength f_{ck}(MPa)	Splitting Strength f_{st} (MPa)	Young's modulus E_c (GPa)	Poisson ratio v_c
Mean	1361	55.94	5.4	15.4	0.25
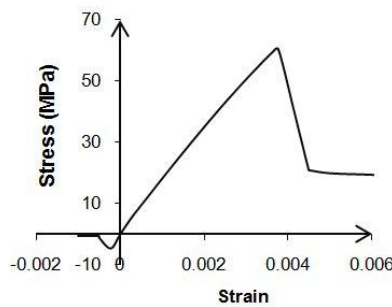
Fig. 5 Stress-strain curves of ULCC
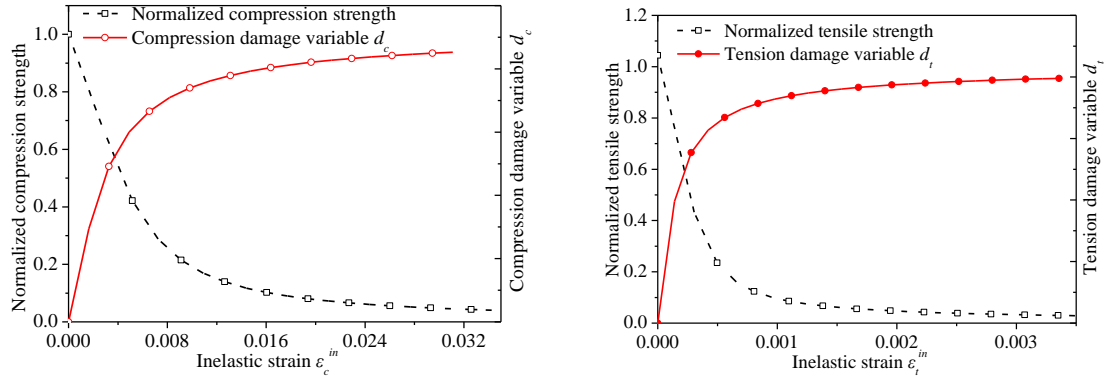
(a) Relationship between compression strength and damage variable v.s. inelastic strain

(b) Relationship between tensile strength and damage variable v.s. inelastic strain

Fig. 6 Concrete damaged plasticity model for ULCC

variable $D_{t,norm}$ and normalised cracking displacement $w_{t,norm}$ can be fitted with a first-order exponential decay function as follows

$$D_{t,norm} = A_1 e^{-w_{t,norm}/t_1} + B_1 \tag{2}$$

where, $D_{t,norm} = d_t$, $w_{t,norm} = w / w_u$, $A_1 = 1/(e^{-1/t_1} - 1)$, $B_1 = -1/(e^{-1/t_1} - 1)$. The only unknown parameter t_1 can be determined by calibrating the load-displacement curves from four-point flexural test results. Using the approaches, the values of the variables t_0 and t_1 for compression and tension damages are estimated to be 0.1 and 0.05 respectively. Fig. 6 illustrates the normalised material parameter of concrete damaged plasticity model for ULCC based on Eqs. (1) and (2).

Besides, in FE analysis, the parameters of concrete grout dilation angle, biaxial/uniaxial ratio, and eccentricity were respectively set as 26.5, 1.16 and 0.1, which were necessary for establishing concrete damage plasticity model (Nguyen and Kim 2009, An *et al*. 2012). A small value of the viscosity parameter, $\kappa = 0.0001$, was used to improve the convergence rate in the concrete following the suggestions from Barth and Wu (2006) and ABAQUS documentation.

3.2.2 Steel face plate and J-hooks

Linear plasticity material model in ABAQUS was utilized to model the stress-strain relationships of the steel material. The corresponding stress-strain relationship of steel face plates and J-hook connectors were obtained from test as shown in Figs. 7 and 8 respectively. The true stress-true strain relationship input in ABAQUS for steel follows the conversion law

$$\sigma = S(1+e) \tag{3}$$

$$\varepsilon = \ln(1+e) \tag{4}$$

where e and S refer to the engineering strain and stress respectively obtained from standard coupon tensile tests, while σ and ε denote the true stress and true strain. Other parameters such as Young's modulus, yield strength and tensile strength of steel plate and J-hook used in FE model are listed in Table 3.

Table 3 Mechanical properties of steel plate and J-hook connectors

Item	Thickness or diameter	E_s (MPa)	f_y (MPa)	f_u (MPa)	v_s
Mild steel plate	6 mm	202.0	309.4	426.8	
	8 mm	179.6	393.9	522.9	0.3
	12 mm	211.5	374.6	507.0	
J-hook bar	φ13 mm	189.9	356.8	521.7	
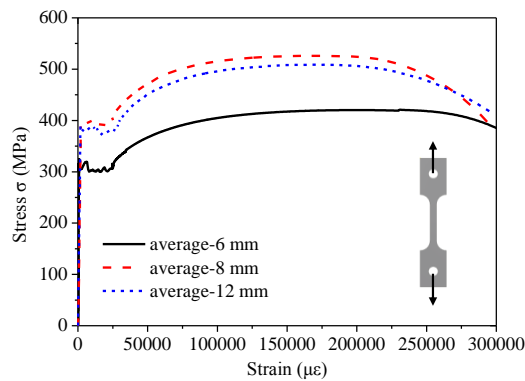
Fig. 7 Stress-strain curves of steel plates with various thickness
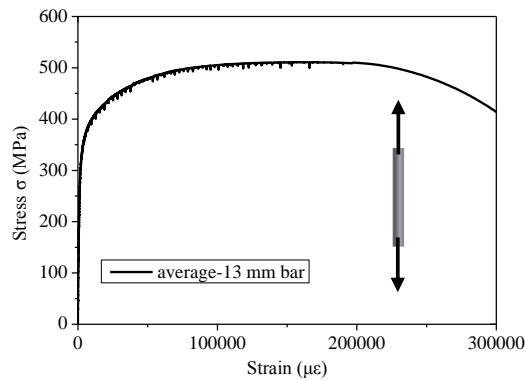
Fig. 8 Stress-strain curves of J-hook bars

3.3 Modelling of J-hook connectors

Recognizing the numerical cost and difficulty to obtain a converged solution, a connector element is used to model the interlocking effect of J-hooks connectors. Each pair of J-hook connectors are modelled using two solid bars connected by a nonlinear connector element as shown in Fig. 9(a). Shear and flexural deformations of the connectors are simulated by the solid bars whereas the connector element is used to emulate only the tensile elongation between the top and bottom connectors. The connector element is coupling at the centre point of both bar section surfaces and a force-displacement relationship may be assigned for the connector element. Tensile

(a) Simplified model for a pair of J-hook connectors

(b) Tensile-elongation of J-hook connector embedded in ULCC (Yan *et al*. 2014)
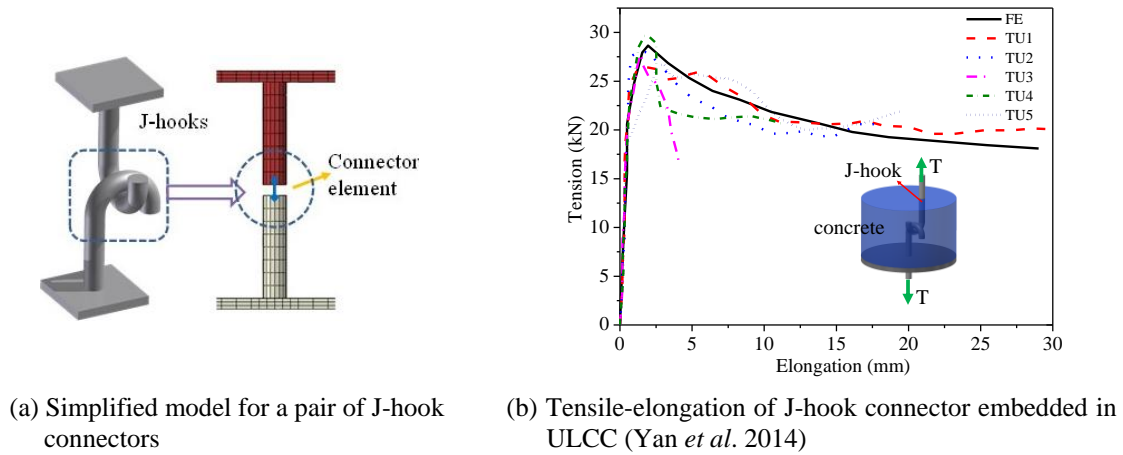
Fig. 9 Simplified connection element for FE modelling

tests are conducted on the double hook connectors embedded in concrete to obtain the tensile force-displacement relationship of J-hook connectors (Sohel *et al*. 2015, Yan *et al*. 2014). The tensile test results used in FE model in this paper are plotted in Fig. 9(b). Moreover, the connector element also considers the fact that the J-hook connectors are aligned eccentrically. Thus, the numbers of contact pairs could be reduced significantly especially when a complicated geometry of contact surfaces are met.

3.4 Wall imperfections

In the FE model, initial geometrical imperfection of the slender wall specimen is considered based on the measured value from the test specimen. The maximum lateral imperfection of a wall can be measured by using three digital inclinometers positioned at both ends and at the location with zero rotation, as shown in Fig. 10.
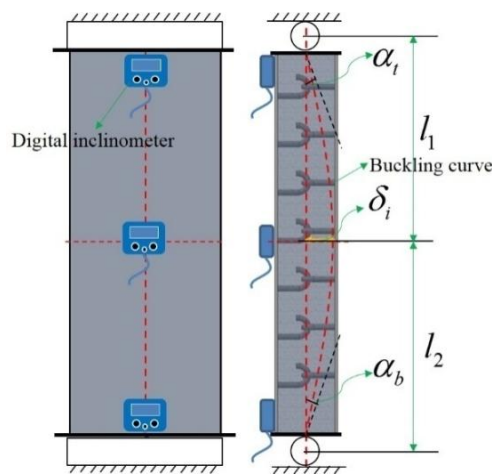

Fig. 10 Imperfection measuring of slender SCS wall

$$\delta_i = \frac{\alpha_t l_1 + \alpha_b l_2}{2} \tag{5}$$

where α_t and α_b are the angle of rotation at the top and bottom of the wall; l_1 and l_2 locate the position of the wall with zero rotation. The FE model is implemented with an initial out-of-straightness represented by the first buckling mode with δ_i as the maximum amplitude based on Eq. (5).

3.5 Solver selection

Implicit and explicit solver is available to conduct the nonlinear FE analysis in ABAQUS. Based on the initial analysis of double skin composite beam and slab when exploring the ABAQUS/Implicit solver, the analysis is challenged by the convergence problem (Shanmugam *et al*. 2002). The reasons may be: (1) nonlinear modelling of concrete in which material (e.g., concrete) suffers severe damage which causing the analysis to diverge at a small proportion of the specified maximum applied load; (2) excessive contacting pairs are introduced or the structures suffer large deformation and highly nonlinear behavior which results in numerical oscillation in FE analysis. The program is terminated immaturely from time to time. Therefore, to successfully conduct FE simulation, on one hand, the material should be accurately modelled. On the other hand, proper calculation technique should be selected. Compared to the implicit solver, explicit solver employing smaller time incensement technique can give a more stable solution rather than consuming a great amount of iterations by using implicit solver so that explicit solver is selected for analyses. Therefore, a quasi-static analysis is defined. For acquiring reliable quasi-static solutions using explicit solver, loading rate should be slow enough to prevent system kinematic energy from being enormous or increasing dramatically compared to total energy in the system. Therefore, different loading rates have been tried and the optimum rate is set to be less than 0.2 mm/s for numerical simulation (Xu and Sugiura 2013).

## 4. Finite element results and discussions

Table 4 compares the maximum loads obtained from FE and test results. The average ratio of is 1.05, with a standard deviation of 0.05. Figs. 11(a)-(g) compare the primary failure modes between FE and test results. The FE results and experimental results are found to match very well. As shown in Fig. 11(a), the concrete crushing and local buckling of steel face plate is captured properly in SCSW-R2. The FE analysis reproduces the concrete damage as observed in the tests. At the concrete core, the dark elements represent elements that have crushed. The predicted damage trend is similar to that observed from tests, but the extent of damage may not the same as that observed from the test, which can be visualized from the figures. The uncertainties associated with concrete at large and post cracking strains are the reasons for occasional differences in the crack patterns. Similar observations are also found in Figs. 11(b)-(d). In Figs. 11(e) and (f), severe local buckling of steel plates in SCSW-S1 and SCSW-S2 are also predicted in accord with the test result. However, it should be noted that the buckling location of steel face plate may not be perfectly predicted due to the unavoidable initial imperfection such as residues stress of steel plate, aggregate imperfection of concrete or initial deboning because of early shrinkage of concrete, vibration during transportation or temperature effect. Nevertheless, the buckling wave could be expectedly captured between the two adjacent shear connectors. For slender sandwich wall SCSW-

Table 4 Comparison of maximum loads between FE and test results

| Specimen	Maximum load		
	P_T (kN)	P_{FE} (kN)	P_T / P_{FE}
SCSW-R1	4191	4295.8	0.98
SCSW-R2	4906	4727.8	1.04
SCSW-H1	4788	4405.1	1.09
SCSW-H2	2975	2826.0	1.05
SCSW-S1	4656	4394.3	1.06
SCSW-S2	3670	3376.7	1.09
SCSW-C1	4248	4013.8	1.06
SCSW-C30	3916	3626.9	1.08
SCSW-C45	4689	4614.1	1.02
SCSW-T8	6889	5939.2	1.16
SCSW-T12	8418	8460.7	0.99
SCSW-P1	5120	5117.1	1.00
SCSW-P2	4933	4636.1	1.06
SCSW-C2	5467	5554.0	0.98
Mean value			1.05
Std. Dev.			0.05
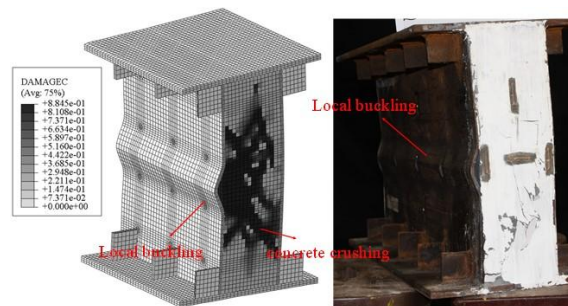

(a) SCSW-R2
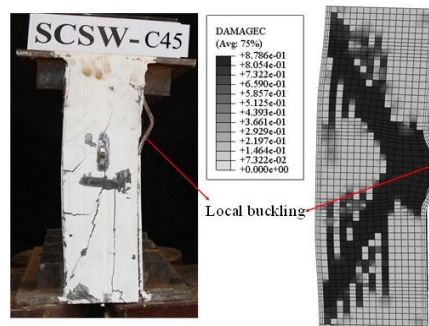
(b) SCSW-C45

Fig. 11 Comparison of failure mode between test and FE results
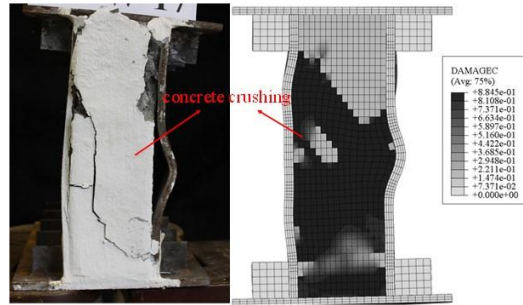
(c) SCSW-T12
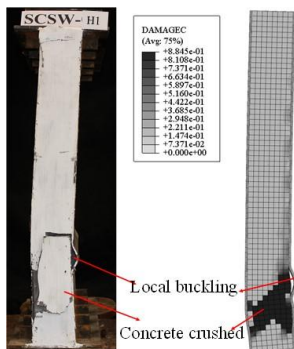
(d) SCSW-H2
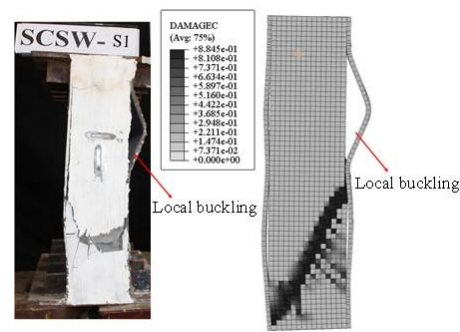
(e) SCSW-S1
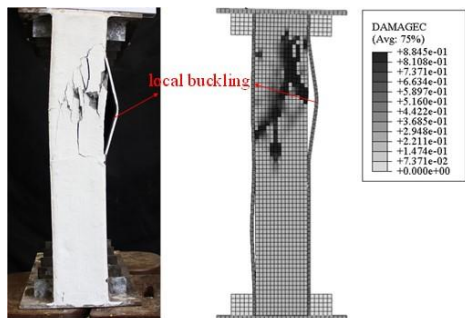
(f) SCSW-S2
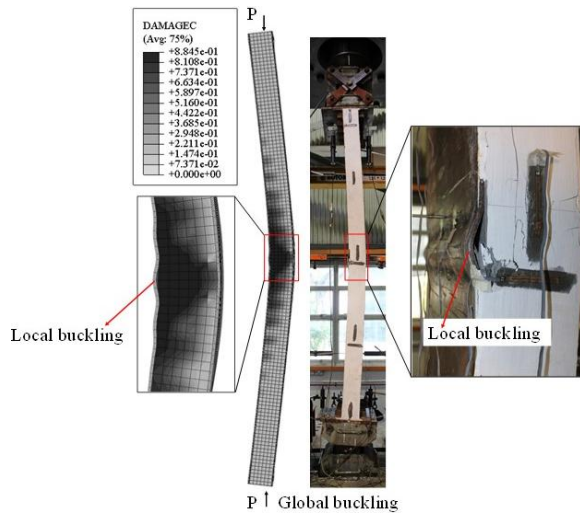
(g) SCSW-H2

Fig. 11 Continued

H2, the proposed FE model also can capture the occurrence of global buckling mode, as shown in Fig. 11(g).

The corresponding load-shortening relations are plotted in Figs. 12(a)-(d). It can be seen that a close agreement between the test and numerical results can be achieved. The FE model also

provides an reasonably accurate estimation on the average strain history at the positions S1 and SG7 for the selected sandwich wall specimens, as demonstrated in Figs. 13(a)-(d). The basic trend of the load-strain curves is similar to that measured from the test.

   In general, the FE analysis in this paper provides close and acceptable estimations on the response for most sandwich wall specimens including the maximum load, the load-shortening curves and the failure modes as well as plate buckling phenomenon. However, after the peak load, the deviation between FE results and test results increases slightly. The FE model may not perfectly capture the post shortening curve behavior, concrete damage zone and buckling location for the reasons that the simplified connector element proposed in this paper ignored the shear effect but only consider the tensile-elongation behavior of J-hook connector. And this reflects the deviation in descending branch of load-shortening curves in Figs. 12(a)-(d). Therefore, a more accurate combined shear-tension interaction model needs to be developed in future study. The developed FE model relies on the basic tension-elongation behavior of the shear connectors embedded in concrete. For different type of shear connectors the tensile tests information should be provided when using the simplified connector element proposed in this paper. For instance, for headed shear studs, the tensile-elongation behavior should be obtained by tensile testing of headed shear studs embedded in concrete. Therefore, further studies should unify a tension or tension-


(a) SCSW-R2   (b) SCSW-S1

(c) SCSW-H1   (d) SCSW-H2
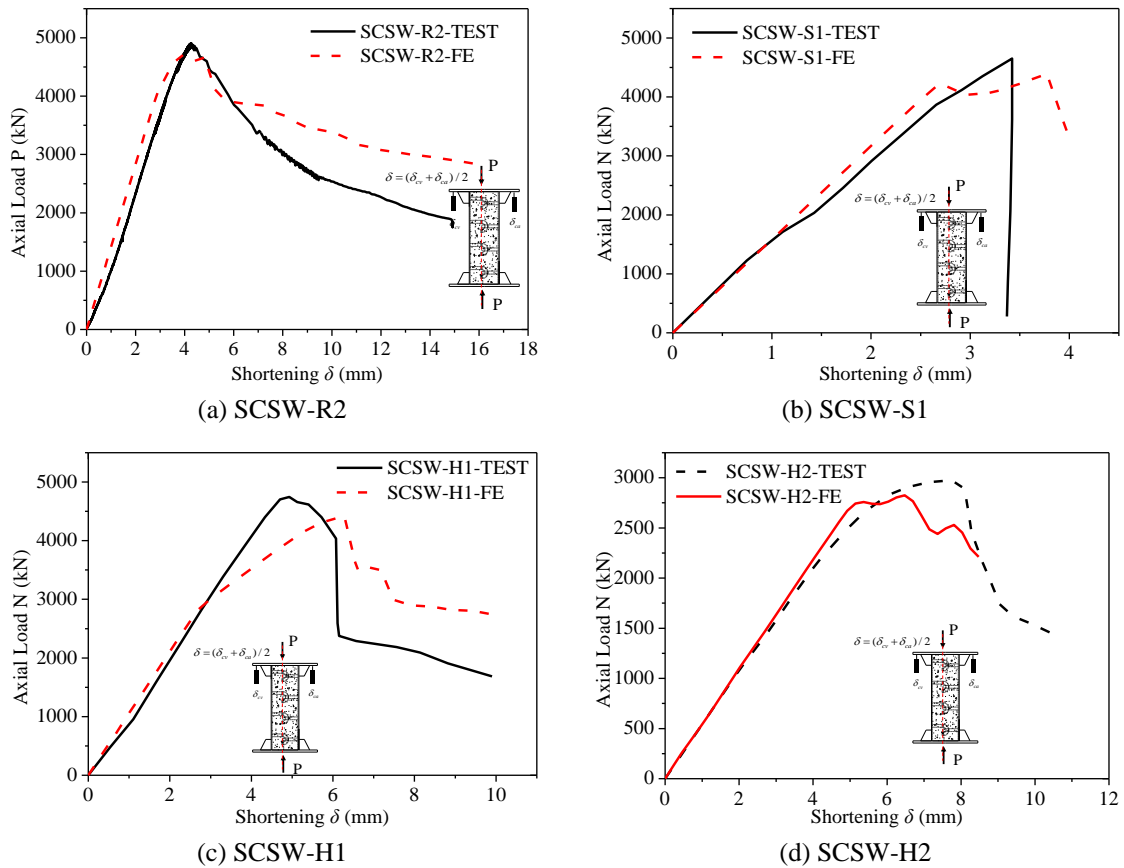
Fig. 12 Comparison of load-shortening curves between test and FE results

(a) SCSW-R2

(b) SCSW-S1

(c) SCSW-H1

(d) SCSW-H2
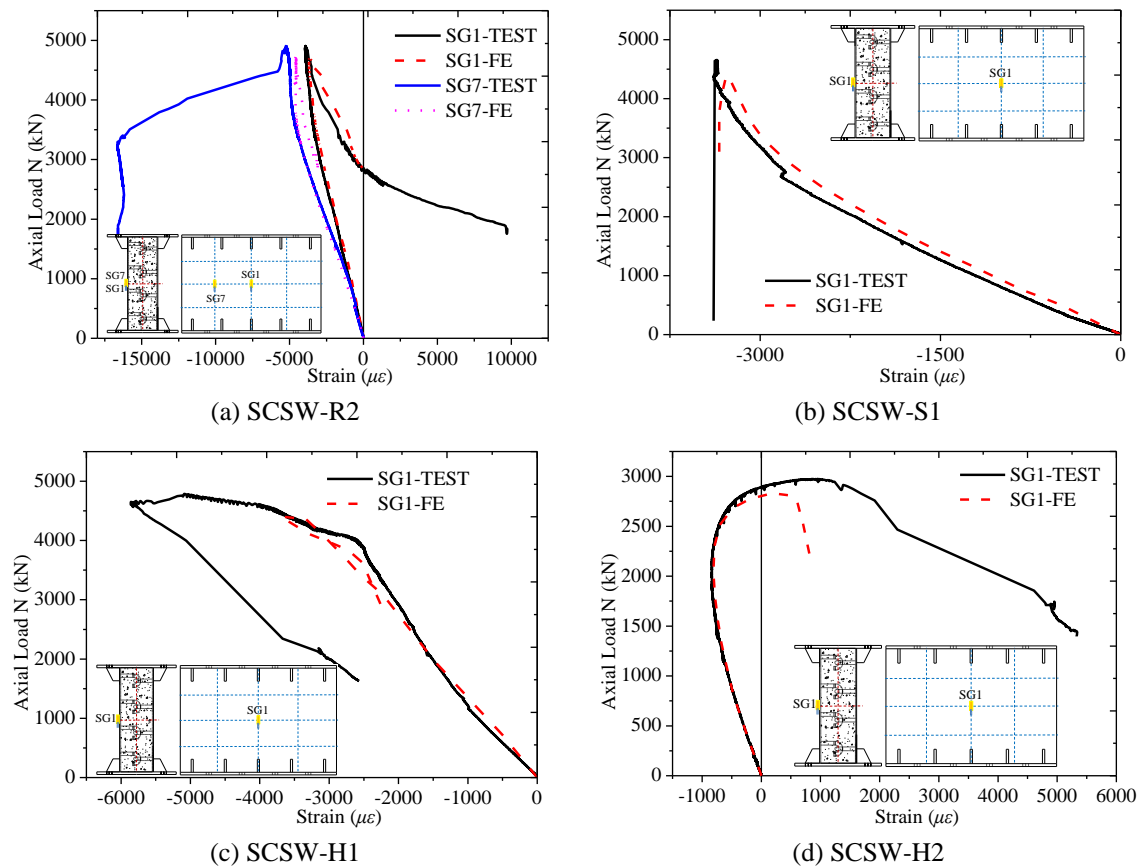
Fig. 13 Comparison of load-strain curves between FE and test results

shear interaction model for different type of shear connectors. Whilst the effect of the bond, shear and tension interaction mechanism between different materials (steel plates and concrete, shear studs and concrete) are very complex and need much further research.

5. Conclusions

A quasi-static finite element analysis using ABAQUS/Explicit programme is performed to investigate the structural behavior of SCS sandwich wall infilled with ultra-lightweight cement composite material. Comparison between the experimental and the numerical results has confirmed the validity of the proposed FE model in analyzing the behavior of the sandwich wall under compressive load. The numerical studies support the following conclusions:

- The main failure modes of SCS sandwich wall under axial compression include (a) concrete core crushing followed by local buckling of steel face plate; (b) local buckling of steel plates only; (c) cross sectional failure and (d) global buckling.
- Through the comparison of the test and FE results, it is demonstrated that the developed FE model is capable of capturing the load-shortening behavior, load-strain curve behavior,

maximum load and the failure modes of SCS sandwich wall with reasonably good accuracy.

The validation studies confirmed the accuracy of proposed FE model over the test results on predicting the compressive behavior of the sandwich wall with novel J-hook connectors. However, the analysis model did not consider the shear effect on the tension-elongation behavior of J-hook connectors. Therefore, it could lead to less-conservative prediction after reaching the peak load. This error would affect post peak unloading branch of the load-shortening curves. More test data are needed to study the combined shear-tension model of J-hook connectors for numerical simulation purpose. The numerical study presented herein path the way for future work to develop design guideline to predict the compressive resistance of steel-concrete-steel sandwich walls.

Acknowledgments

References

Abaqus 6.13 Online Documentation (2013), Abaqus Analysis User's Manual © Dassault Systèmes, Hibbit, Karlsson and Sorensen, Inc., RI, USA.

Aboobucker, M.A.M., Wang, T.Y. and Richard Liew, J.Y. (2009), "An experimental investigation on shear bond strength between steel and fresh cast concrete using epoxy", *IES J Part A*: *Civil Struct. Eng.*, **2**(2), 107-115.

Barth, K.E. and Wu, H.Y. (2006), "Efficient nonlinear finite element modeling of slab on steel stringer bridges", *Finite. Elem. Anal. Des.*, **42**(14-15), 1304-1013.

An, C., Castello, X., Duan, M., Filho, R.D.T. and Estefen, S.F. (2012), "Ultimate strength behavior of sandwich pipes filled with steel fiber reinforced concrete", *Ocean. Eng.*, **55**, 125-135.

Choi, B.J., Kang, C.K. and Park, H.Y. (2014), "Strength and behavior of steel plate-concrete wall structures using ordinary and eco-oriented cement concrete under axial compression", *Thin-Wall. Struct.*, **84**, 313-324.

Dabaon, M., El-Khoriby, S., El-Boghdadi, M. and Hassanein, M.F. (2009), "Confinement effect of stiffened and unstiffened concrete-filled stainless steel tubular stub columns", *J. Constr. Steel. Res.*, **65**(8), 1846-1854.

Epackachi, S., Whittaker, A.S. and Huang, Y.N. (2015), "Analytical modeling of rectangular SC wall panels", *J. Constr. Steel. Res.*, **105**, 49-59.

Hu, H.S. and Nie, J.G. (2015), "Numerical study of concrete-filled steel plate composite coupling beams", *Thin-Wall. Struct.*, **96**, 139-154.

Huang, Z.Y. and Liew, J.Y.R. (2015), "Nonlinear finite element modelling and parametric study of curved steel–concrete–steel double skin composite panels infilled with ultra-lightweight cement composite", *Constr. Build. Mater.*, **95**, 922-938.

Huang, Z.Y. and Liew, J.Y.R. (2016a), "Structural behaviour of steel-concrete-steel sandwich composite wall subjected compression and end moment", *Thin-Wall. Struct.*, **98**, 592-606.

Huang, Z.Y. and Liew, J.Y.R. (2016b), "Compressive resistance of steel-concrete-steel sandwich composite walls with J-hook connectors", *J. Constr. Steel. Res*. DOI: 10.1016/j.jcsr.2016.05.001

Huang, Z.Y., Liew, J.Y.R., Xiong, M.X. and Wang, J.Y. (2015a), "Structural behavior of double skin composite system using ultra-lightweight cement composite", *Constr. Build. Mater.*, **86**, 51-63.

Huang, Z.Y., Wang, J.Y., Liew, J.Y.R. and Marshall, P.W. (2015b), "Lightweight steel–concrete–steel sandwich composite shell subject to punching shear", *Ocean. Eng.*, **102**, 146-161.

Li, W., Han, L.H. and Chan, T.M. (2014), "Numerical investigation on the performance of concrete-filled double-skin steel tubular members under tension", *Thin-Wall. Struct.*, **79**, 108-118.

Liew, J.Y.R. and Sohel, K.M.A. (2009), "Lightweight steel–concrete–steel sandwich system with J-hook connectors", *Eng. Struct.*, **31**(5), 1166-1178.

Liew, J.Y.R. and Wang, T.Y. (2011), "Novel steel-concrete-steel sandwich composite plates subject to impact and blast load", *Adv. Struct. Eng.*, **14**(4), 673-687.

Liew, J.Y.R., Koh, C.G. and Sohel, K.M.A. (2009), "Impact tests on steel–concrete–steel sandwich beams with lightweight concrete core", *Eng. Struct.*, **31**(9), 2045-2059.

Long, Y.L. and Cai, J. (2013), "Stress–strain relationship of concrete confined by rectangular steel tubes with binding bars", *J. Constr. Steel. Res.*, **88**, 1-14.

Marshall, P.W., Sohel, K.M.A., Liew, J.Y.R., Yan, J.B., Palmer, A.C. and Choo, Y.S. (2012), "Development of SCS sandwich composite shell for Arctic Caissons", *Proceedings of Offshore Technology Conference*, Paper No. 23818, Houston, TX, USA, December.

Nguyen, H.T. and Kim, S.E. (2009), "Finite element modeling of push-out tests for large stud shear connectors", *J. Constr. Steel. Res.*, **65**(10-11), 1909-1920.

Remennikov, A.M. and Kong, S.Y. (2012), "Numerical simulation and validation of impact response of axially-restrained steel-concrete-steel sandwich panels", *Comp. Struct.*, **94**(12), 3546-55.

Remennikov, A.M., Kong, S.Y. and Uy, B. (2013), "The response of axially restrained noncomposite steel-concrete-steel sandwich panels due to large impact loading", *Eng. Struct.*, **49**, 806-818.

Seifi, R. and Abbasi, K. (2015), "Friction coefficient estimation in shaft/bush interference using finite element model updating", *Eng. Fail. Anal.*, **57**, 310-322.

Shanmugam, N.E., Kumar, G. and Thevendran, V. (2002), "Finite element modelling of double skin composite slabs", *Finite. Elem. Anal. Des.*, **38**(7), 579-599.

Smitha, M.S. and Kumar, S.R.S. (2013), "Steel-concrete composite flange plate connections-finite element modeling and parametric studies", *J. Constr. Steel. Res.*, **82**, 164-176.

Sohel, K.M.A. and Liew, J.Y.R. (2011), "Steel–concrete–steel sandwich slabs with lightweight core-static performance", *Eng. Struct.*, **33**(3), 981-992.

Sohel, K.M.A. and Liew, J.Y.R. (2014), "Behavior of steel–concrete–steel sandwich slabs subject to impact load", *J. Constr. Steel. Res.*, **100**, 163-175.

Sohel, K.M., Liew, J.Y.R. and Koh, C.G. (2015), "Numerical modelling of lightweight Steel-Concrete-Steel sandwich composite beams subjected to impact", *Thin-Wall. Struct.*, **94**, 135-146.

Wang, J.C. and Chen, Y.K. (2006), *Application of ABAQUS in Civil Engineering*, Zhejiang University Press, Hangzhou, P.R. China.

Wang, Y.Y., Yang, Y.L. and Zhang, S.M. (2012), "Static behaviors of reinforcement-stiffened square concrete-filled steel tubular columns", *Thin-Wall. Struct.*, **58**, 18-31.

Xie, M., Foundoukos, N. and Chapman, N.C. (2004), "Experimental and numerical investigation on the shear behavior of friction-welded bar-plate connections embedded in concrete", *J. Constr. Steel. Res.*, **61**(5), 625-649.

Xu, C. and Sugiura, K. (2013), "Parametric push-out analysis on group studs shear connector under effect of bending-induced concrete cracks", *J. Constr. Steel. Res.*, **89**, 86-97.

Yan, J.B., Liew, J.Y.R and Zhang, M.H. (2014), "Tensile resistance of J-hook connectors used in Steel-Concrete-Steel sandwich structure", *J. Constr. Steel. Res.*, **100**, 146-162.

Zhang, K., Varma, A.H., Malushte, S.R. and Gallocher, S. (2014), "Effect of shear connectors on local buckling and composite action in steel concrete composite walls", *Nucl. Eng. Des.*, **269**, 231-239.

Zheng, Y., Robinson, D., Su, T. and David, C. (2009), "Finite element investigation of the structural behavior of deck slabs in composite bridges", *Eng Struct.*, **31**(8), 1762-1776.

CC